HOKKAIDO UNIVERSITY

Title	Effect of pyrolysis kinetic parameters on the overload ignition of polymer insulated wires in microgravity
Author(s)	Guo, Feng; Kawaguchi, Seiya; Hashimoto, Nozomu et al.
Citation	Proceedings of The Combustion Institute, 39(3), 3939-3947 https://doi.org/10.1016/j.proci.2022.08.087
Issue Date	2023
Doc URL	https://hdl.handle.net/2115/93266
Rights	© <2023>. This manuscript version is made available under the CC-BY-NC-ND 4.0 license http://creativecommons.org/licenses/by-nc-nd/4.0/
Rights(URL)	https://creativecommons.org/licenses/by-nc-nd/4.0/
Type	journal article
File Information	Guo_PROCI_39(3)_3939-3947.pdf

Hokkaido University Collection of Scholarly and Academic Papers : HUSCAP

Effect of pyrolysis kinetic parameters on the overload ignition of polymer insulated wires in microgravity

Feng Guo*, Seiya Kawaguchi, Nozomu Hashimoto, Osamu Fujita*

Division of Mechanical and Space Engineering, Hokkaido University, Kita 13, Nishi 8, Kita-ku, Sapporo, Hokkaido, 060-8628, Japan

---

Abstract

The overload ignition of polymer insulated wires in microgravity was investigated as basic information for space fire safety. This paper focuses on the effect of pyrolysis kinetic parameters of the insulation material on the ignition characteristics. A two-dimensional numerical model calculation under varied pyrolysis model was carried out to simulate the overload ignition, and microgravity experiments have been conducted for the model validation. With the help of thermogravimetric analysis, the original pyrolysis model of the polyethylene insulation used for wire ignition experiments was obtained. Three groups of varied pyrolysis models were proposed by changing the activation energy (E), pre-exponential factor (A) from the original model. Numerical simulations were conducted with the varied pyrolysis models. The simulated results employing the original pyrolysis model showed a good agreement with the microgravity experiments for ignition delay time with continuous current and the minimum ignition energy (MIE) with short-term current, respectively. From the simulation results with continuous overloading, the independent variation of A and E in the pyrolysis model has a limited effect on the ignition delay time but a significant effect on ignition modes in microgravity. Such effects are mainly reflected by changing the pyrolysis temperature during overloading, which determines the ease of spontaneous ignition. With a constant pyrolysis temperature, the change of mass loss rate in the pyrolysis model may affect the transition point from the "spontaneous ignition" to the "wire assisted ignition" when the current increases. Finally, for short-term current supply in microgravity, the single change of A or E showed higher MIE than the original pyrolysis model.

Keywords: Space fire safety; Ignition; Electric wire; Microgravity; Pyrolysis.

---

*Corresponding author.

E-mail address: ofujita@eng.hokudai.ac.jp (O. Fujita), cumt-guofeng@hotmail.com (F. Guo)

1. Introduction

In spacecraft, overloads and short circuits in electrical wires could pose a potential fire hazard for space exploration activities [1,2]. Therefore, research on the ignition of overloaded wires in microgravity is important to provide fundamental understandings for space fire safety.

Ignition of solid materials in microgravity has been extensively studied to prevent fires in space, like radiative ignition of thin cellulosic sheets [3–7] and piloted ignition of polymethyl methacrylate (PMMA) samples [8–10]. When it comes to the wire ignition in microgravity, effects of external heat sources [11,12] and smoke emission by overloading [13–15] were studied experimentally.

Previously, our research group has conducted a series of experimental and numerical works on the overload ignition of polyethylene (PE) insulated wires in microgravity [16–19]. Dramatic extensions of ignition limits have been found in microgravity under continuous [16] and short-term current supply [17]. To predict ignition phenomena beyond the time limits of ground-based microgravity experiments, a one-dimensional (1-D) numerical model has been developed for overload ignition in microgravity [18,19]. Takano [18] has reported a nearly constant minimum ignition energy (MIE) of overloaded wires with short-term applied currents. Shimizu [19] has pointed out the importance of radiant heat loss from the wire surface in near ignition limit conditions with continuous current supply. Recently, we proposed an upgraded 2-D numerical model utilizing the Fire Dynamic Simulator (FDS) to optimize the prediction of overload ignition, which showed a better consistency with experimental results compared with the previous 1-D model [20,21].

As a candidate experiment of the "FLARE" project to be conducted in the International Space Station [22,23], long-term ignition tests of overloaded wires will include more applied scenarios, where the impacts of different insulation materials are of interest. Polymeric materials for the wire insulation always have different pyrolysis characteristics affecting the overload ignition in different ways. Even for the same kind of polymer, such as PE, the pyrolysis kinetic parameters are always different in literature [24]. Compared with the pyrolysis heat and other thermophysical properties, the effect of pyrolysis kinetic parameters on the overload ignition process are always not straightforward. To clarify such complex coupling effect, parametric studies are needed by controlling sub-models of pyrolysis and combustion in the numerical model.

In the present work, we will focus on the effect of pyrolysis kinetic parameters on the overload ignition using the 2-D numerical model. As PE insulated wire samples in previous experiments were adopted from the same producer, the original pyrolysis model can be derived by thermogravimetric analysis (TGA) as a baseline. The pyrolysis kinetic parameters will be varied to clarify their impacts on overload ignition in microgravity.

2. Experimental and numerical methods

The experimental setup was identical to the previous microgravity experiments by drop tower and parabolic flights [16,17], which included a sealed combustion chamber with a wire sample, a direct current power supply system, and an image recording system through the windows. The wire sample was 70 mm in length, with the nichrome (NiCr) core wire of 0.5 mm in diameter and the low-density polyethylene (LDPE) insulation of 0.15 mm thickness. The ignition time was determined by hi-speed imaging method with synchronizing the onset of microgravity, current supply and recording. Detailed experimental methods can be found in a previous paper [17]. The schematic of the experimental chamber is shown in the left part of Fig. 1.

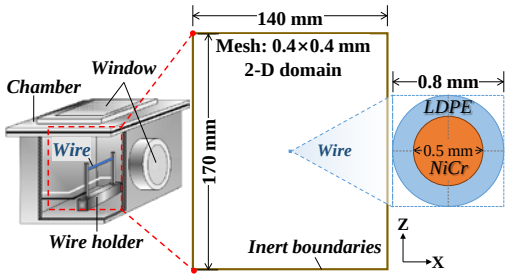

Fig. 1. Schematic of the experimental chamber and the 2-D numerical model.

The 2-D numerical model was developed utilizing FDS ver. 6.7.1 [25,26]. As illustrated in Fig. 1, the 2-D model was taken from the cross-section of the experimental chamber under a Cartesian coordinate system. The mesh size was set as 0.4×0.4 mm to achieve a balance of computation time and simulation accuracy in LES mode, the resolution sensitivity was analyzed in the supplementary material (S1). The initial time step was set as 0.001 s, and it was automatically adjusted during the simulation to constrain the Courant number below 0.8.

The wire located at the center of the domain was assumed as infinite long, which has a layered surface boundary condition. Although the geometric appearance of the wire matches with the rectilinear mesh, the surface boundary was set as cylindrical with a diameter of 0.8 mm and an outer layer thickness of 0.15 mm. The heat conduction equations in the solid and boundary conditions including the empirical convection model on the surface and mass flux in the pyrolysis model follow the cylindrical coordinates. As wire samples used in experiments are very thin (on mm-scale), we assume that the conformance to the rectilinear mesh has a limited effect on the ignition phenomena. The inner core material is NiCr with an electric resistance of 5.5 Ω/m, which produced Joule

heat under different current supplies. The outer layer material is LDPE as the wire insulation. The melting process was simulated by setting the temperature (391 K) and enthalpy of melting (140.6 kJ/kg [27]) using the simplified phase change reaction model without considering the dripping process [26]. To facilitate modeling the gas-phase combustion reaction, the pyrolysis of LDPE was assumed as a single-step reaction to produce 100% monomers of ethylene (C_2H_4), which was adopted by related numerical works as well [18,19]. The pyrolysis reaction rate was expressed as an Arrhenius form:

$$r_s = A(\rho_s/\rho_{s0})\exp(-E/RT_s) \quad (1)$$

where r_s is the pyrolysis reaction rate (s^{-1}), A is the pre-exponential factor (s^{-1}), ρ_s is the density of the insulation material (kg/m^3), E is the activation energy (J/mol), R is the gas constant (8.314 J/K/mol), and T_s is the temperature of the insulation material (K). The kinetic parameters were obtained from the TGA in the following section. The heat of pyrolysis (excluding sensible heat) for LDPE is 962 kJ/kg from the reference [28]. The other physical properties were listed in Table 1, where data for NiCr core and solid-phase LDPE were taken from the datasheet provided by the manufacturer of our wire samples (DAIYU Electric Wire Co., Ltd.). It is worth noting that the emissivity of LDPE insulation is thickness-dependent, smaller than 0.4 when the thickness is smaller than 0.2 mm [29], which is much smaller than the bulk (~0.9) [30]. According to the previous experimental observation [7], the increased transparency of molten LDPE may lead to a lower emissivity. Therefore, smaller value of emissivity was adopted for the thin LDPE melts.

Table 1
Physical properties of materials for the solid phase model.

Properties \ Materials	NiCr	LDPE solid	LDPE melts
Density (kg/m^3)	8410	920	760 [31]
Specific heat (kJ/kg/K)	0.481	2.3	2.5 [32]
Thermal conductivity (W/m/K)	17.4	0.34	0.25 [33]
Emissivity (-)	0.7	0.3 [34]	0.1 [35]

In the gas phase, the Finite-Rate Chemistry model was utilized, where the single-step 1.75 order reaction scheme of C_2H_4 combustion was employed referring to the work of Westbrook and Dryer [36]:

$$d[C_2H_4]/dt = -A_g\exp(-E_g/RT_g)[C_2H_4]^{0.1}[O_2]^{1.65} \quad (2)$$

where gas-phase activation energy (E_g) is 125520 J/mol (30 kcal/mol), the gas-phase pre-exponential factor (A_g) is 2.0×10^{12} $(mol/cm^3)^{-0.75}s^{-1}$, T_g is the gas-phase temperature, $[C_2H_4]$ and $[O_2]$ are mole concentrations of fuel and oxygen, respectively.

The initial condition and boundary conditions on the wire surface are consistent with the previous numerical works [18,19], but the outer boundaries were set as inert wall at the ambient temperature without mass transfer. The ambient temperature is 293 K, the ambient oxygen fraction is 21 vol%, and the pressure is 1 atm with zero gravity (0G).

The critical local reaction rate has been considered an adequate ignition criterion for solid materials under wide investigations by Kashiwagi and Nakamura [5,37,38], which is equivalent to the critical volumetric heat release rate (HRRPUV) and basically the same as the thermal explosion theory. By calculating the critical HRRPUV using Equation (2) at the autoignition temperature of C_2H_4 (815 K [39]) under the stoichiometric condition with air, the ignition criterion here was determined by the HRRPUV reaching 32 MW/m^3. The magnitude of this value is also consistent with the ignition criterion suggested for solid material combustion [5,10]. By computing the 2-D transport phenomena and local gas-phase reaction, the ignition point could be observed by visualizing the HRRPUV data on a 2-D slice.

3. TGA and pyrolysis models

Figure 2 shows the TGA results of the LDPE insulation material used for microgravity experiments. The normalized mass changes (m/m_0) with the temperature rise are at the top of the figure, and the corresponding mass-loss rates (MLR/m_0) are at the bottom figure. The TGA experiments were conducted in the pure nitrogen atmosphere under different heating rates, 1, 3 and 10 K/min. The TGA curves indicate the single-step thermal decomposition of the typical non-charring material. The faster heating rate led to a higher reference temperature of pyrolysis (T_p). The pyrolysis model was derived using the Kissinger method for the first approximation [40], then modifying the A and E to compare the calculated results from FDS with the experiments for the best fitting, as shown by the lines in Fig. 2. The obtained pyrolysis model was regarded as the reference, named original model, for the following parametric studies.

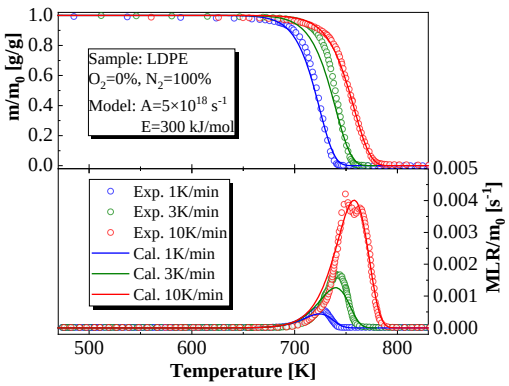

Fig. 2. Experimental and calculated TGA data obtained for LDPE insulation at heating rates of 1, 3 and 10 K/min.

In general, the A and E variation affect the typical temperatures and the reaction rate of the pyrolysis. According to the database collected by Witkowski [24] and Stoliarov [30], pyrolysis temperatures (with peak MLRs) of most polymers are in the range of 600-900 K under the heating rate of 10K/min. To cover this wide range of pyrolysis temperatures, the variations of the pyrolysis models for the parametric studies were categorized into three groups, as listed in Table 2. Besides separately varying the A and E, the third group was designed for a constant T_p at the 10 K/min heating rate with different MLRs. The simulated derivative thermogravimetric (DTG) curves of three groups compared with the original model were plotted in Fig. 3. A and E show a similar effect of shifting the T_p during the heating condition, and the pyrolysis is more sensitive to the change of E than A. When considering the scenarios of the overloaded wire with LDPE insulation, the difference in T_p indicates the difference of released gas temperature by overloading; the peak MLR affects the instantaneous velocity of the pyrolysis gas; meanwhile, the width of the DTG curve implies the duration of pyrolysis.

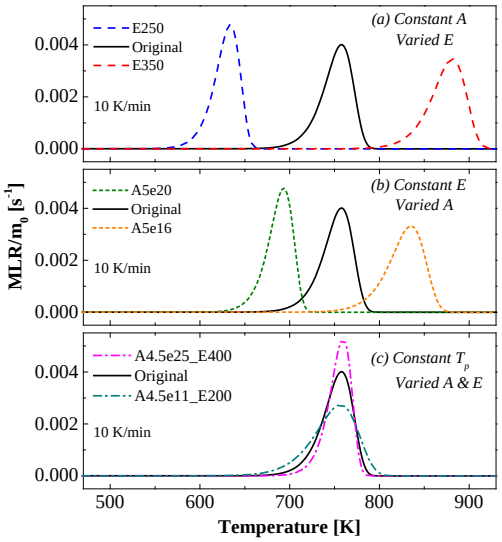

Fig. 3. Comparison of DTG curves at the heating rate of 10 K/min between the original model and models with varied parameters: (a) Constant A with varied E, (b) Constant E with varied A, and (c) Constant T_p with different MLRs by varying A and E combinations.

Table 2
Kinetic parameters and designations of pyrolysis reaction models used for the 2D simulations.

Reaction models	A (s^{-1})	E (kJ/mol)	T_p (K) at 10K/min
Original pyrolysis model			
Original	5.0×10^{18}	300	760
Constant *A*, varied *E*			
E250	5.0×10^{18}	250	633
E350	5.0×10^{18}	350	882
Constant *E*, varied *A*			
A5e20	5.0×10^{20}	300	693
A5e16	5.0×10^{16}	300	835
Constant T_p, varied *A* and *E*			
A4.5e25_E400	4.5×10^{25}	400	760
A4.5e11_E200	4.5×10^{11}	200	760

4. Results and discussions

4.1 Validation by microgravity experiments

Figure 4 shows the typical ignition process of overloaded wire in microgravity under continuous current supply. The release of pyrolysis gas can be observed at 2.987 s, then the ignition occurred away from the wire and the consequent flame showed a cylindrical shape due to the absence of buoyancy.

Figure 5 shows results of ignition characteristics as a function of applied current, including ignition delay time (t_{ig}), radial ignition position (R_{ig}), and the ratio of the ignition delay time to the pyrolysis completion time (t_{ig}/t_p). In Fig. 5 (a), the simulation results with the original pyrolysis model show a good agreement with the microgravity experiments. Due to the time limit of ground-based microgravity experiments (typically shorter than 20 s), no ignition was found when the applied current was lower than 3 A. In addition, with the applied current of 8A, the R_{ig} (~12 mm) and the t_{ig}/t_p (<1) also qualitatively agreed with the experimental ignition phenomena (flame size and existence of wire insulation) in Fig. 4. These validated simulation results could be the baseline for reference. Therefore, further parametric studies will compare the simulated results between the original pyrolysis model and its variants.

4.2 Effect of activation energy change

Figure 5 also compared ignition characteristics with the constant A and varied E in the pyrolysis model. Overall, the variation of E did not change the t_{ig} significantly. E250 with smaller activation energy shows a longer t_{ig} under a lower current supply. By contrast, the R_{ig} (defined as the radial distance from the center to the initiation point exceeding the ignition criteria) differs in the cases with different E values. As reported by our recent work employing the original pyrolysis model [20], there were two ignition modes in terms of ignition position, the "spontaneous ignition" appeared away from the wire, and "wire assisted ignition" initiated from the wire surface. With the applied current increase, the ignition mode shifted from the "spontaneous ignition" to the "wire assisted ignition" around 15 A, as shown by the black curve with open circle plots in Fig. 5 (b). Different from the behavior of the original model, E250 shows the "wire-assisted ignition" throughout current range, while E350 always results in the "spontaneous ignition". In Fig. 5 (c), the ratio of t_{ig}/t_p indicates the competition

of gas-phase reaction and solid-phase pyrolysis. The t_{ig}/t_p of E250 is always greater than one, which means the core wire exposure before ignition; however, the t_{ig}/t_p of E350 keeps smaller than one, confirming that the "spontaneous ignition" controlled by the hot pyrolysis gas.

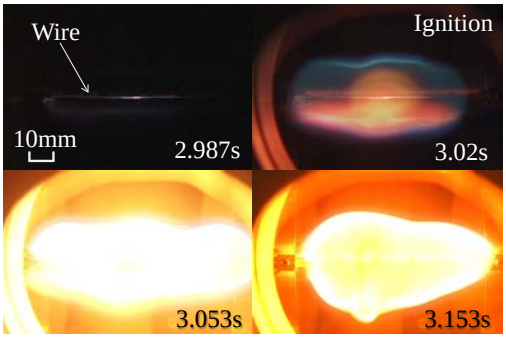

Fig. 4. Typical overload ignition process of LDPE insulated wire in microgravity experiments (O_2=21%, 8 A, continuous current supply).

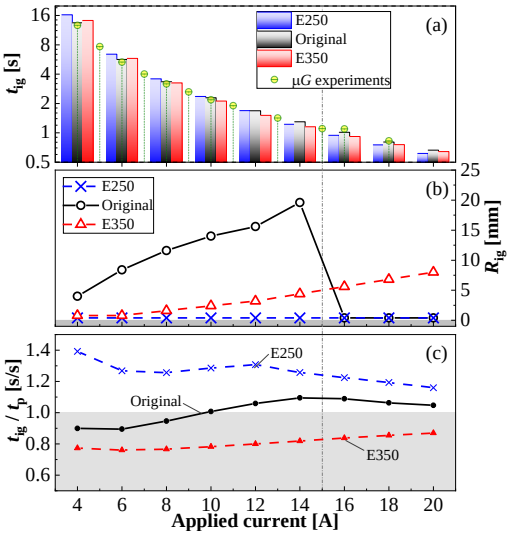

Fig. 5. Results of ignition characteristics as a function of applied current with the constant A (5.0×10^{18} s^{-1}) and varied E in the pyrolysis model.

To clarify why the varied E gave different ignition modes, we selected the typical scenario under 10 A continuous current supply in 0G for comparison, where the R_{ig} and t_{ig}/t_p results from the three models differ clearly. Figure 6 shows time-dependent changes wire surface temperature, core temperature and the C_2H_4-O_2 mass fraction adjacent to the wire surface. Under the same current supply, three models with different E had the same rate of temperature rise at the early period until the pyrolysis. When the E increased by 50 kJ/mol, the pyrolysis temperature rose more than 100 K. In the reference case at 10 A employing the original model, ignition started right after the pyrolysis finished. The anaerobic condition made it impossible to ignite at the wire surface, and the spontaneous ignition could only have been caused by the exothermic reaction of pyrolyzed gas. By comparison, although the E250 with a smaller E makes the pyrolysis easier, the low pyrolysis temperature (~700 K) can hardly lead to a spontaneous ignition. After completion of pyrolysis, the wire surface temperature became identical to the core temperature, and it increased dramatically; meanwhile, the local O_2 fraction gradually increased by inward diffusion, as shown by the blue dashed line in Fig. 6. The exposed core wire with excessive heat acted as a piloted ignition source leading the "wire-assisted ignition". In general, E350 with a larger E can be regarded as a better thermal stability. However, under 10 A overloading in 0G, the higher pyrolysis temperature gave sufficient heat to the released C_2H_4, which cause the "spontaneous ignition" at the early period of pyrolysis.

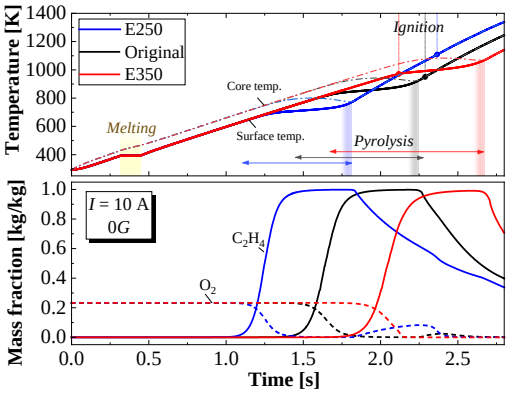

Fig. 6. Histories of wire surface temperature, core temperature and C_2H_4-O_2 mass fractions adjacent to the wire surface under the applied current of 10 A in 0G. Comparing the simulation results with the constant A (5.0×10^{18} s^{-1}) and varied E in the pyrolysis model.

4.3 *Effect of pre-exponential factor change*

Figure 7 shows ignition characteristics (t_{ig}, R_{ig}, and t_{ig}/t_p) as a function of applied current, comparing the results between the original pyrolysis model and the models with varied A. As discussed in Fig. 3, the effect of the pre-exponential factor in the pyrolysis model is similar to the activation energy. The A5e20 with a larger A led to a longer ignition delay, especially in the case of low current supply. The results of t_{ig}/t_p by A5e20 and A5e16 show a similar trend with Fig. 5. The larger A makes the ignition always happen after the core exposure, while the smaller A always leads to the spontaneous ignition. However, the simulated ignition position from A5e20 shows a different trend, ignition was found away from the wire surface when the applied current was between 8A to 12A. To clarify whether this "far-distance" ignition belongs to the "spontaneous ignition" mode, Figure 8 shows the volumetric heat

release rate (HRRPUV) distributions in the gas phase along with the radial direction from the wire center. Besides the ignition moment, three important moments before the ignition were plotted as well.

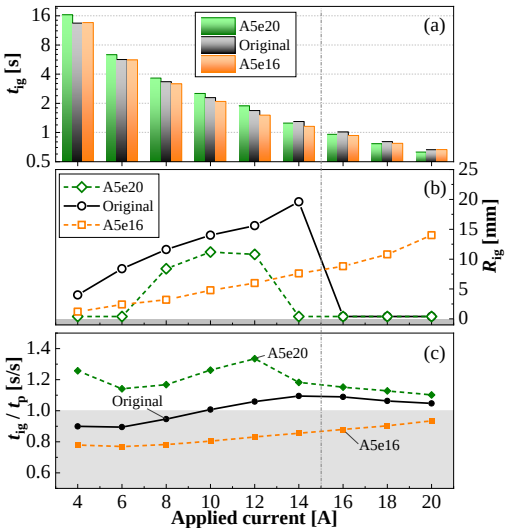

Fig. 7. Simulation results of ignition characteristics as a function of applied current with the constant E (300 kJ/mol) and varied A in the pyrolysis model.

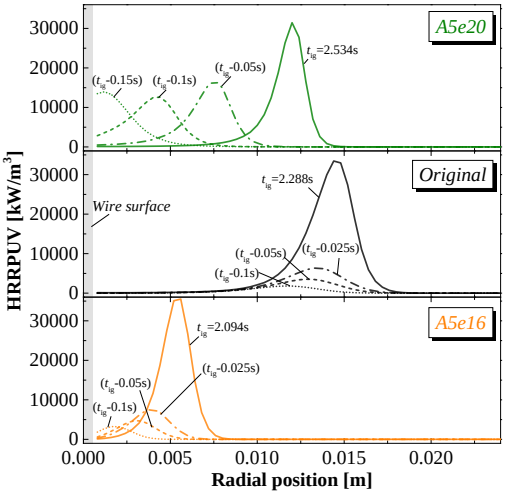

Fig. 8. Development of HRRPUV distribution in radial direction until the ignition moments under 10 A current supply. Comparing the simulation results with the constant E (300 kJ/mol) and varied A in the pyrolysis model.

From the reference case employing the original model in Fig. 8, the exothermic reaction was initiated at 12 mm from the wire surface, while the pyrolysis process was not finished yet. With the pyrolyzed gas diffused outward, the gas-phase thermal runaway led to the sudden increase of HRRPUV to the ignition criteria within 0.1 s. On the other hand, the results of A5e16 are similar to E350. The high-temperature gas released in the early stage of pyrolysis diffuses slowly, which causes the spontaneous ignition closer to the wire. However, A5e20 shows different distributions of HRRPUV before ignition. As the pyrolysis ended at 2 s, the outward movement of the heat release is not likely attributed to the diffusion of pyrolyzed gas. The hot surface of the exposed wire assisted the exothermic reaction near the wire with insufficient oxygen, then the reactive front propagated outward until reaching the ignition criteria. Therefore, even it behaves as a far-distance ignition, its nature still belongs to the "wire assisted ignition" mode. Additional data with gas temperature, velocity and reactant species distributions were presented in the supplementary material (S2).

4.4 Effect of MLR change with the constant T_p

Figure 9 shows ignition characteristics as a function of applied current, comparing the results between the original pyrolysis model and the models with the same T_p and different MLRs. Similarly, the MLR change in the pyrolysis model has a limited effect on the t_{ig} but affects the tendency of the ignition position varied with the applied current. Combining R_{ig} and t_{ig}/t_p results, the t_{ig}/t_p values are all less than one at a lower current level, which results in the spontaneous ignition; while with the applied current increase, each t_{ig}/t_p grows sequentially to a value greater than one. Correspondingly, the ignition mode switched with the same order. Therefore, the MLR change in the pyrolysis model may affect the transition point from the "spontaneous ignition" to the "wire assisted ignition" when the current increases. Such minor effect is mainly reflected the pyrolysis duration and the instantaneous velocity of the pyrolyzed gas.

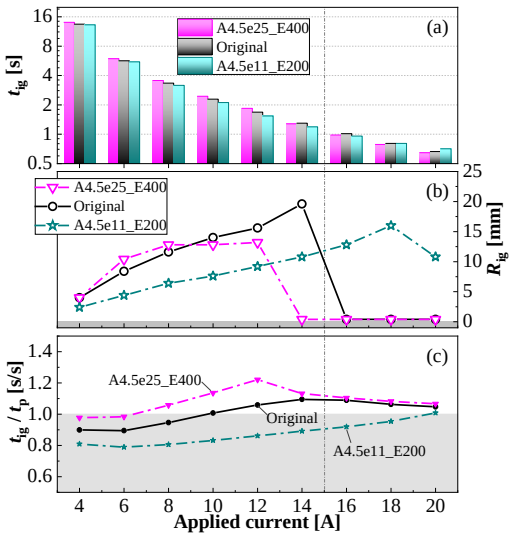

Fig. 9. Simulation results of ignition characteristics as a function of applied current with the constant T_p and different MLRs in the pyrolysis model.

4.5 Impacts on the minimum ignition energy with short-term current

Previous subsections have discussed the effects of pyrolysis kinetic parameters on the ignition of overloaded wire under continuous current supply in microgravity. Here, we will consider their impact on the ignition of overloaded wire with the short-term current to mimic the scenario of short circuits in microgravity. The supply of short-term current follows the pattern in the previous works [17]. As the MIE in microgravity under short-term current is almost independent of the applied time [17,18], we just select a single applied time of 1 s for the comparative analysis with different pyrolysis models.

Figure 10 shows the ignition map and MIE with 1s applied current in microgravity for experimental and numerical results employing different pyrolysis models. In Fig. 10 (a), each symbol represents one trial of the experiment or simulation. The circle means ignition while the cross means non-ignition. The size of the circle represents the ignition delay time. From the ignition map with 1s current supply, the experimental limit is between 13 to 14 A. The original model successfully reproduced the experimental conditions and narrowed the ignition limit to 13.2A. The t_{ig} values near the limit are all more than 1 s, and they decrease with the current increase.

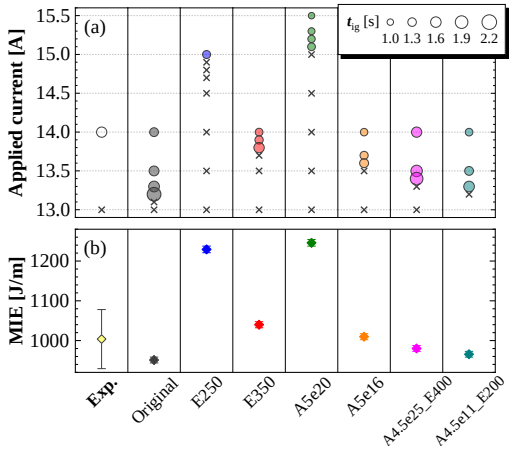

Fig. 10. Effect of pyrolysis model on the wire ignition with a short-term (1 s) current supply. (a) Ignition map at different applied current (b) Minimum ignition energy.

In Fig. 10 (b), the MIE from each pyrolysis model was calculated as the averaged value between the nearest ignition and non-ignition conditions with the error bars. For models of E250 and A5e20 with lower T_p, the MIE is much more than the experimental and original simulated MIE. In addition, they all led to a wire-assisted ignition even in the short-term case. As the T_p are too low to cause the spontaneous ignition, they need more energy to consume all the PE and heat the core wire to give a piloted ignition. For models of E350 and A5e16 with higher T_p, the MIE is slightly higher, because the high threshold of pyrolysis required more energy to heat the material to a certain temperature. Finally, for the models with the same T_p, the MIE is very close to the MIE from the original pyrolysis model.

5. Concluding remarks

Overload ignition of polymer insulated wires in microgravity was investigated under experimental and numerical approaches to find the effect of pyrolysis kinetic parameters of the insulation material. The original pyrolysis model of LDPE insulation used for wire ignition experiments was obtained from TGA experiments. The original and varied pyrolysis models were employed in the 2-D numerical to simulate the wire ignition in microgravity. The main concluding remarks are as follows.

(1) The 2-D numerical model employing the original pyrolysis model reproduce the overload ignition phenomena in microgravity, which showed a good agreement with the experimental results in terms of ignition delay time and MIE under continuous and short-term current, respectively.
(2) The independent variation of the activation energy and the pre-exponential factor in the pyrolysis model has a limited effect on the ignition delay time but significantly affects the ignition modes in microgravity. The effect is mainly reflected by changing the pyrolysis temperature, which determines the ease of spontaneous ignition. It means that, for example, if we apply the wire insulation material with high activation energy for space use, we have a higher risk of spontaneous ignition.
(3) With a constant pyrolysis temperature, the change of MLR in the pyrolysis model may affect the transition point from the “spontaneous ignition” to the “wire assisted ignition” when the current increases.
(4) The independent variations of the activation energy and the pre-exponential factor in the pyrolysis model can increase the MIE under the short-term (1 s) current supply in microgravity.

In future work, the charring, solid oxidation, and different decomposition products will be considered in the numerical study to step-by-step increase the complexity. Under the cross-validation with long-term microgravity test on ISS, the framework to design a fire-safe material for the space environment is expected.

Acknowledgements

This research was supported by JAXA as a candidate experiment for the third stage use of JEM/ISS titled “Evaluation of gravity impact on combustion phenomenon of solid material toward higher fire safety” (called “FLARE”).

Supplementary material

Supplementary material associated with this article can be found.

References

[1] R. Friedman, Fire Safety in Spacecraft, *Fire Mater.* 20 (1996) 235–243.

[2] X. Huang, Y. Nakamura, A Review of Fundamental Combustion Phenomena in Wire Fires, *Fire Technol.* 56 (2020) 315–360.

[3] T. Kashiwagi, K.B. McGrattan, S.L. Olson, O. Fujita, M. Kikuchi, K. Ito, Effects of slow wind on localied radiative ignition and transition to flame spread in microgravity, *Symp. Combust.* 26 (1996) 1345–1352.

[4] O. Fujita, J. Takahashi, K. Ito, Experimental study on radiative ignition of a paper sheet in microgravity, *Proc. Combust. Inst.* 28 (2000) 2761–2767.

[5] Y. Nakamura, H. Yamashita, T. Takeno, G. Kushida, Effects of gravity and ambient oxygen on a gas-phase ignition over a heated solid fuel, *Combust. Flame*. 120 (2000) 34–48.

[6] J. Takahashi, O. Fujita, K. Ito, The effect of irradiation angle on laser ignition of cellulose sheet in microgravity, *Proc. Combust. Inst.* 30 II (2005) 2311–2317.

[7] S.. L. Olson, T. Kashiwagi, O. Fujita, M. Kikuchi, K. Ito, Experimental observations of spot radiative ignition and subsequent three-dimensional flame spread over thin cellulose fuels, *Combust. Flame*. 125 (2001) 852–864.

[8] S. McAllister, C. Fernandez-Pello, D. Urban, G. Ruff, Piloted ignition delay of PMMA in space exploration atmospheres, *Proc. Combust. Inst.* 32 (2009) 2453–2459.

[9] S. McAllister, C. Fernandez-Pello, D. Urban, G. Ruff, The combined effect of pressure and oxygen concentration on piloted ignition of a solid combustible, *Combust. Flame*. 157 (2010) 1753–1759.

[10] Y. Nakamura, T. Kashiwagi, Effects of sample orientation on nonpiloted ignition of thin poly(methyl methacrylate) sheet by a laser, *Combust. Flame*. 141 (2005) 149–169.

[11] Y. Kobayashi, Y. Konno, X. Huang, S. Nakaya, M. Tsue, N. Hashimoto, O. Fujita, C. Fernandez-Pello, Laser piloted ignition of electrical wire in microgravity, *Proc. Combust. Inst.* 37 (2019) 4211–4219.

[12] M. Nagachi, F. Mitsui, J.-M. Citerne, H. Dutilleul, A. Guibaud, G. Jomaas, G. Legros, N. Hashimoto, O. Fujita, Effect of Ignition Condition on the Extinction Limit for Opposed Flame Spread Over Electrical Wires in Microgravity, *Fire Technol.* 56 (2020) 149–168.

[13] K. Wang, B.R. Wang, Y.H. Ai, W.J. Kong, Study on the pre-ignition characteristics of wire insulation in the narrow channel setup, *Sci. China Technol. Sci.* 55 (2012) 2132–2139.

[14] S. Xue, W. Kong, Smoke emission and temperature characteristics of the long-term overloaded wire in space, *J. Fire Sci.* 37 (2019) 99–116.

[15] J.-F. Guan, J. Fang, Y. Xue, J.-W.J. Wang, J.-W.J. Wang, Y.-M. Zhang, Morphology and concentration of smoke from fluorinated ethylene propylene wire insulation in microgravity under forced airflow, *J. Hazard. Mater.* 320 (2016) 602–611.

[16] K. Agata, O. Fujita, Y. Ichimura, T. Fujii, H. Ito, Y. Nakamura, Wire Insulation Ignition with Excess Electric Current in Microgravity, *J. Japan Soc. Microgravity Appl.* 25 (2008) 11–16.

[17] O. Fujita, T. Kyono, Y. Kido, H. Ito, Y. Nakamura, Ignition of electrical wire insulation with short-term excess electric current in microgravity, *Proc. Combust. Inst.* 33 (2011) 2617–2623.

[18] Y. Takano, O. Fujita, N. Shigeta, Y. Nakamura, H. Ito, Ignition limits of short-term overloaded electric wires in microgravity, *Proc. Combust. Inst.* 34 (2013) 2665–2673.

[19] K. Shimizu, M. Kikuchi, N. Hashimoto, O. Fujita, A numerical and experimental study of the ignition of insulated electric wire with long-term excess current supply under microgravity, *Proc. Combust. Inst.* 36 (2017) 3063–3071.

[20] S. Kawaguchi, F. Guo, N. Hashimoto, O. Fujita, Difference of ignition characteristics of long-term overloaded electric wire between microgravity and normal gravity, in: 13th Asia-Pacific Conf. Combust. 2021, Abu Dhabi, UAE, 2021.

[21] F. Guo, S. Kawaguchi, N. Hashimoto, O. Fujita, Effect of gravity on the ignition of polyethylene insulated wire with continuous excess current supply, in: 13th Asia-Pacific Conf. Combust. 2021, Abu Dhabi, UAE, 2021.

[22] O. Fujita, Introduction of JAXA Priority Project FLARE utilizing ISS/"KIBO", *Int. J. Microgravity Sci. Appl.* 32 (2015) 1–5.

[23] O. Fujita, Solid combustion research in microgravity as a basis of fire safety in space, *Proc. Combust. Inst.* 35 (2015) 2487–2502.

[24] A. Witkowski, A.A. Stec, T.R. Hull, Thermal Decomposition of Polymeric Materials, in: SFPE Handb. Fire Prot. Eng., Springer New York, New York, NY, 2016: pp. 167–254.

[25] K. McGrattan, S. Hostikka, R. McDermott, J. Floyd, M. Vanella, Fire Dynamics Simulator User's Guide, Gaithersburg, MD, 2018.

[26] K.B. McGrattan, S. Hostikka, J. Floyd, M. Vanella, Fire Dynamics Simulator Technical Reference Guide Volume 1: Mathematical Model, Gaithersburg, MD, 2018.

[27] J. Brandrup, E.H. Immergut, E.A. Grulke, Polymer Handbook, 4th ed., Wiley, 2003.

[28] A. Tewarson, R.F. Pion, Flammability of plastics—I. Burning intensity, *Combust. Flame*. 26 (1976) 85–103.

[29] Y. Fujikura, T. Suzuki, M. Matumoto, POLYMER EMISSIVITY, *Sen'i Gakkaishi*. 31 (1975) T381–T388.

[30] S.I. Stoliarov, N. Safronava, R.E. Lyon, The effect of variation in polymer properties on the rate of burning, *Fire Mater.* 33 (2009) 257–271.

[31] R. Dray Mfg. Inc. of Texas, Melt Density, (2017).

[32] W.N. dos Santos, Thermal properties of melt polymers by the hot wire technique, *Polym. Test.* 24 (2005) 932–941.

[33] M.Y. Keating, C.S. Mclaren, Thermal conductivity of polymer melts, *Thermochim. Acta*. 166 (1990) 69–76.
[34] T. Okada, R. Ishige, S. Ando, Analysis of Thermal Radiation Properties of Polyimide and Polymeric Materials Based on ATR-IR spectroscopy, *J. Photopolym. Sci. Technol.* 29 (2016) 251–254.
[35] Optotherm Support, Emissivity in the Infrared, (2018). https://www.optotherm.com/emiss-table.htm.
[36] C.K. Westbrook, F.L. Dryer, Simplified Reaction Mechanisms for the Oxidation of Hydrocarbon Fuels in Flames, *Combust. Sci. Technol.* 27 (1981) 31–43.
[37] T. KASHIWAGI, A Radiative Ignition Model of a Solid Fuel, *Combust. Sci. Technol.* 8 (1973) 225–236.
[38] Y. NAKAMURA, T. TAKENO, Appropriate Criterion of Spontaneous Ignition of an Externally Heated Solid Fuel in Numerical Study, *JSME Int. J. Ser. B.* 44 (2001) 288–298.
[39] I. Glassman, R. Yetter, Spontaneous ignition temperature data, in: Combustion, Elsevier, 2015: pp. 705–729.
[40] A.C.Y. Yuen, T.B.Y. Chen, G.H. Yeoh, W. Yang, S.C.-P. Cheung, M. Cook, B. Yu, Q.N. Chan, H.L. Yip, Establishing pyrolysis kinetics for the modelling of the flammability and burning characteristics of solid combustible materials, *J. Fire Sci.* 36 (2018) 494–517.